Proceedings of the American Control Conference
Arlington, VA June 25-27, 2001

Modeling and Controller Design of an Electromagnetic Engine Valve[†]

Chun Tai, Andrew Stubbs*, Tsu-Chin Tsao

Department of Mechanical and Aerospace Engineering
University of California, Los Angeles

ABSTRACT

A control-oriented linear model was constructed for an electromagnetic camless valvetrain (EMCV) based on a gray-box approach that combines mathematical modeling and system identification. An inner-loop feedback stabilizing controller and a cycle-to-cycle repetitive learning feedforward controller were designed for the EMCV to meet the quiet-seating requirement. The performance of this control system is demonstrated by experimental results.

INTRODUCTION

Electromagnetic Camless Valvetrain (EMCV) offers potential for making a high-performance engine. However, the quite-seating issue must be solved before commercializing this product. This means that a control system is required to maintain the seating speed below a given level. A simple way to do this is to give a series of open-loop pulses to the electromagnetic actuator. The problem of using open-loop pulses is that since the open-loop system is unstable, the valve response is sensitive to perturbation and suffers poor repeatability. As we tune the pulse-widths such that the seating velocity becomes smaller and smaller, the valve might sometimes not close at all, which is totally unacceptable. To make sure that the valve will close every time, we have to endure the hitting velocity above some level. The seating velocity is limited below 0.05 m/s in camshaft design. Our system repeatability test shows that the lowest seating velocity we may achieve without any failure (i.e. the valve does not close at all) is 0.2-0.5 m/s, which is quite higher than what can be achieved by camshaft. [4]

The poor open-loop valve motion repeatability suggests that feedback control be applied to reduce the sensitivity. It takes two steps to address this problem. The first step is to develop a model of the EMCV system. In 2000 Wang *et al* [9] published their EMCV model. During the same year Stubbs [4] created his model independently in his master's thesis. Both of these models are rather reasonable and complete, except that they did not consider the dynamic effect of lash, which connects the armature and engine valve. The purpose of putting a lash between the armature and engine valve is to achieve smooth contact and allow for thermal expansion effect. At low frequency, we may ignore the dynamic effect of lash by replacing the lash with a rigid connection. However, the frequency range we are interested in is pretty high due to the requirement of fast seating. In this paper we present an EMCV model with consideration of the lash effect and demonstrate the necessity of including this effect in the model.

[†] This research was supported in part by Ford Motor Company.
Corresponding author's email: ttsao@seas.ucla.edu.

* Department of Mechanical and Industrial Engineering, University of Illinois, Urbana-Champaign

The second step to address this problem is to design controller based upon the model achieved from the first step. In 2000 Butzmann *et al* [1] published their control algorithm and experimental results on this issue. By using the current measurement only, the seating velocities they achieved for the laboratory test bench were below 0.1m/s, which is quite remarkable. The control proposed in this paper consists of an inner-loop linear output feedback controller and a cycle-to-cycle repetitive learning controller. It takes valve position measurement as the feedback signal. We limited our maximum supply voltage to be 42V because that would be the maximum voltage available on a vehicle in the future. [1] Our goal is to control the seating velocity below 0.05 m/s for most of the engine cycles.

1. SYSTEM MODELING

The EMCV system consists of two electric magnets, an armature, two springs, a lash and an engine valve. The armature moves between the two magnets. When neither magnet is energized the armature is held at the mid-point of the two magnets by the two springs located on either side of the armature. This system is then used to control the motion of the engine valve. The engine valve is then in turn used to control the flow of air into and out of a combustion engine cylinder. [4]

For valve closing, we need to energize the upper coil in figure 1. The relationship between current i and force F is given by:

$$F = \frac{K_l i^2}{(G_l - X_1)^2} \qquad \text{(eq. 1-1)}$$

where K_l and G_l are two parameters that need to be identified from the experimental system. [4] If we linearize this equation within a

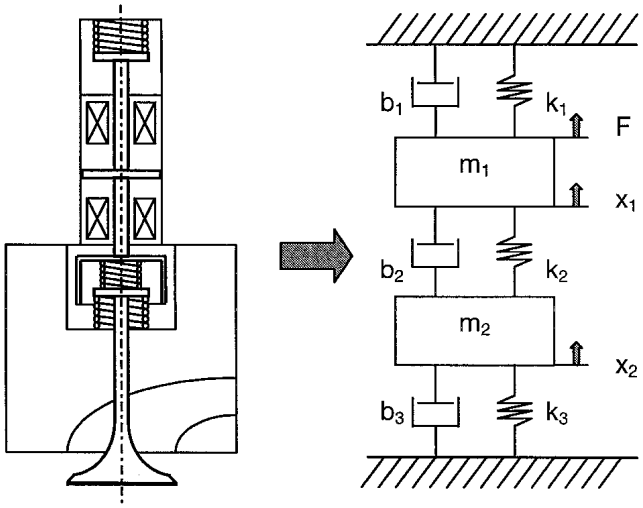

Figure 1. Schematic of the EMV system

small range of X_1, we get

$$dF = G_1 \cdot dX_1 + G_2 \cdot di \qquad \text{(eq. 1-2)}$$

where

$$G_1 = \frac{2K_I i^2}{(G_I - X_1)^3} \qquad \text{(eq. 1-3)}$$

$$G_2 = \frac{2K_I}{(G_I - X_1)^2}$$

For small range of X_1, we assume that G_1 and G_2 are two constants. For the mechanical part, we have

$$\begin{bmatrix} m_1 s^2 + (b_1 + b_2)s + (k_1 + k_2) & -b_2 s - k_2 \\ -b_2 s - k_2 & m_2 s^2 + (b_2 + b_3)s + (k_2 + k_3) \end{bmatrix} \begin{bmatrix} X_1 \\ X_2 \end{bmatrix} = \begin{bmatrix} F \\ 0 \end{bmatrix} \qquad \text{(eq. 1-4)}$$

By combining eq. 1-2 and eq. 1-4, we have

$$\begin{bmatrix} m_1 s^2 + (b_1 + b_2)s + (k_1 + k_2 - G_1) & -b_2 s - k_2 \\ -b_2 s - k_2 & m_2 s^2 + (b_2 + b_3)s + (k_2 + k_3) \end{bmatrix} \begin{bmatrix} dX_1 \\ dX_2 \end{bmatrix} = \begin{bmatrix} G_2 di \\ 0 \end{bmatrix} \qquad \text{(eq. 1-5)}$$

$$\begin{bmatrix} dX_1 \\ dX_2 \end{bmatrix} = \frac{G_2 \cdot \begin{bmatrix} m_2 s^2 + (b_2 + b_3)s + (k_2 + k_3) \\ b_2 s + k_2 \end{bmatrix} \cdot di}{(m_1 s^2 + (b_1 + b_2)s + (k_1 + k_2 - G_1))(m_2 s^2 + (b_2 + b_3)s + (k_2 + k_3)) - (b_2 s + k_2)^2} \qquad \text{(eq. 1-6)}$$

Therefore, the small-signal transfer function from current i to position X_2 have four poles and one zero.

$$\frac{dX_2}{di} = \frac{G_2 \cdot (b_2 s + k_2)}{(m_1 s^2 + (b_1 + b_2)s + (k_1 + k_2 - G_1))(m_2 s^2 + (b_2 + b_3)s + (k_2 + k_3)) - (b_2 s + k_2)^2} \qquad \text{(eq. 1-7)}$$

To predict where the four poles roughly are, we simplify the characteristic equation by assuming b_1 and b_2 to be zero. This gives us:

$$(m_1 s^2 + (k_1 + k_2 - G_1))(m_2 s^2 + (k_2 + k_3)) - k_2^2 = 0 \qquad \text{(eq. 1-8)}$$

After reformulating this equation we have:

$$1 + k_2 \cdot \frac{((m_1 + m_2)s^2 + (k_1 + k_3 - G_1))}{(m_1 s^2 + (k_1 - G_1))(m_2 s^2 + k_3)} = 0 \qquad \text{(eq. 1-9)}$$

Note that k_2 (due to the lash) is much larger than the spring constants k_1 and k_3. The transfer function may or may not be stable, depending on how "strong" the negative spring G_1 is. If $G_1 < k_1$, then we have four lightly damped stable poles in our transfer function. If $G_1 > (k_1 + k_3)$, then we have one unstable pole on the real axis. If $k_1 < G_1 < (k_1 + k_3)$, then it further depends on the value of k_2 whether we are going to have an unstable pole or not. Large k_2 tends to make the transfer function stable (see Figure 2).

System identification tests were conducted on the experimental system to extract the unknown parameters in our model. The open-loop plant turned out to be unstable. Therefore, we had to stabilize the plant first, and then conduct the system identification test under the closed-loop system. Pseudo-random-binary-signal (PRBS) was used as the excitation signal. Data were recorded around four different valve positions (see Figure 3). The distances of the regulated position to the seating position of these four runs are 0.01, 0.28, 0.50, and 0.66 mm, respectively. By matching with the experimental data, we parameterize our plant model (from control voltage to valve position) as following:

$$G(s) = \frac{K(\tau s + 1)}{\left(\frac{s^2}{\omega_1^2} + \frac{2\zeta_1 s}{\omega_1} - 1\right) \cdot \left(\frac{s^2}{\omega_2^2} + \frac{2\zeta_2 s}{\omega_2} + 1\right)} \qquad \text{(eq. 1-10)}$$

This identified transfer function has two lightly damped stable poles, one stable real pole, and one unstable real pole (see Figure 3). It confirms the model we derived before (the case *b* or case *c* in Figure 2). It is also apparent from Figure 3 that the nonlinearity of this plant (variation of static gain at different valve position) is significant.

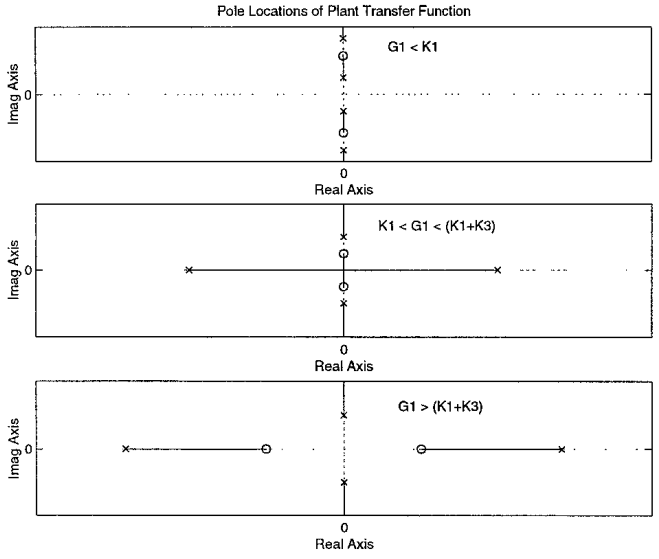

Figure 2. Possible Plant Poles Locations

(a) $G_1 < k_1$, (b) $k_1 < G_1 < (k_1 + k_3)$, (c) $G_1 > (k_1 + k_3)$

2. TRAJECTORY DESIGN

It is shown by our system repeatability test that the lowest

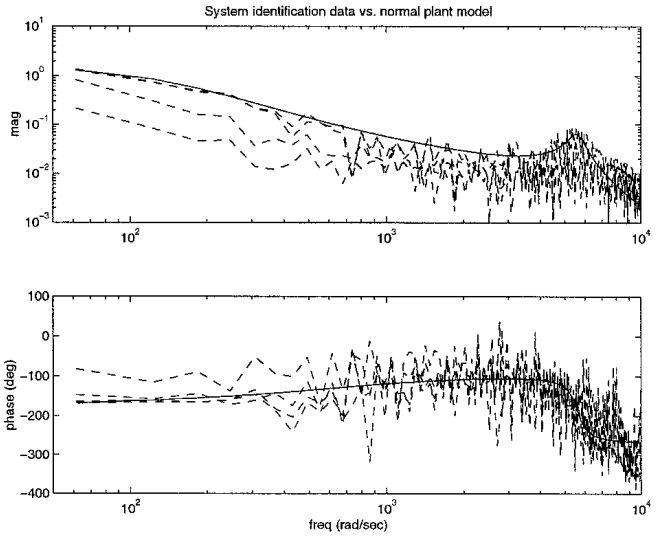

Figure 3. System Identification and Curve Fitting

seating velocity we may achieve by pure feedforward control is 0.2-0.5 m/s. [4] If we want to further reduce the seating speed, we have to rely on a feedback control system. We may use an open-loop pulse to drag the engine valve down to some position close to the valve seat, and then start closed-loop control to force the valve to track some desired trajectory with low seating speed. The closed-loop control could reduce the sensitivity of seating velocity to unknown perturbations. Therefore, it could make the engine valve shut off every time with smaller seating velocity.

In Figure 4, the dotted line shows the valve trajectory by using an open-pulse only. Here we tune this open-loop pulse such that it drags the valve very close to the seating position and yet without touching. The trajectory we designed for the valve to track is shown in Figure 4, line segment b-c. Figure 4 is a state-space plot, and on this plot the designed trajectory is a straight line that is tangent to the open-loop trajectory. The connecting point of the two trajectories is the point for us to start the closed-loop control. There are two reasons for us to choose this trajectory. Firstly, define the slope of the trajectory

$$s = \frac{dv}{dx} = \frac{dv/dt}{dx/dt} = \frac{a}{v} = f(i, v, x) \qquad \text{(eq. 2-1)}$$

We know that although the voltage could change almost instantaneously, the coil current i can only change continuously with respect to time due to the existence of coil inductance. Therefore, the slope of the valve trajectory on the state-space plot is a continuous function. This acts as a constraint to the trajectory design that any designed trajectory should be tangent to the open-loop trajectory on the state-space plot.

Secondly, it is desired for the engine valve to follow a trajectory to the closing position fast and yet insensitive to unknown disturbance. If we take a look at Figure 4, the points in the area below line a-b indicates faster movement but are more sensitive to unknown perturbation; and the points above line b-c are less sensitive to perturbation, but give slower valve movement. Thus, the straight-line b-c is a balanced trajectory between moving speed and sensitivity to perturbations. In time-domain this trajectory is an exponential curve. We end up with a trajectory similar to what Butzmann *et al* [1] used.

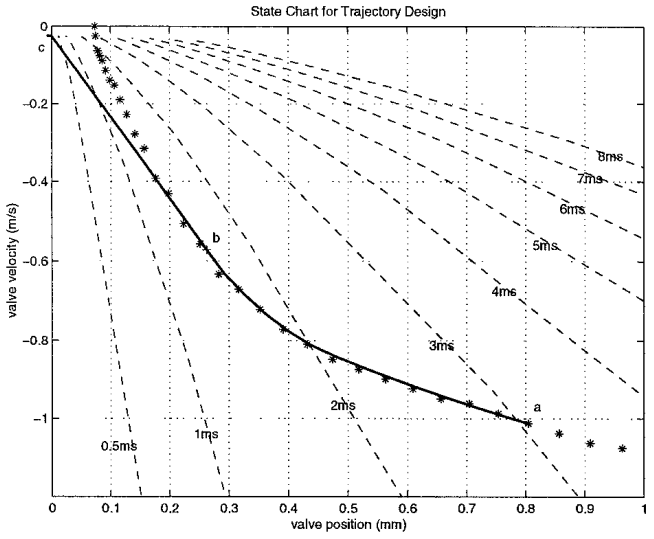

Figure 4. State-Space Plot for Trajectory Design

Following is the trajectory design procedure. Let y stand for the valve position, t stand for time, and v stand for valve velocity, i.e. the derivative of y. Then

$$y(t) = a \cdot \exp(bt) + c \qquad \text{(eq. 2-2)}$$

This trajectory starts from y_0 at $t_0 = 0$, and reaches the nominal wall position $y_f = 0$ at $t = t_f$ with seating velocity v_f. With given boundary conditions:

$$y(0) = y_0,\ \dot{y}(0) = v_0,\ y(t_f) = 0,\ \dot{y}(t_f) = v_f$$

we can solve for the unknown parameters a, b, c, and the seating time t_f.

$$a = \frac{y_0 v_0}{v_0 - v_f}$$

$$b = \frac{v_0 - v_f}{y_0} \qquad \text{(eq. 2-3)}$$

$$c = \frac{y_0 v_f}{v_f - v_0}$$

$$t_f = \frac{y_0}{(v_0 - v_f)} \log\left(\frac{v_f}{v_0}\right)$$

Eq. 2-3 tells us the relationship between initial valve position and velocity we chose and the seating velocity and seating time we are going to get based upon this trajectory design method. Figure 4 also shows some constant seating-time lines with given initial conditions and the desired seating velocity of 25mm/sec. These lines can be used to choose the initial conditions for seating control from the open-loop trajectory.

In the actual implementation, we started our feedback control from point *a* instead of point *b* on Figure 4. The desired trajectory for the valve to track from point *a* to point *b* is just the trajectory generated by our open-loop pulse. This means that ideally the output of the feedback controller would be zero all the way along point *a* to point *b*. The reason for doing this is that later if we want to implement repetitive learning control, the feedforward signal needs to start a little bit earlier than the feedback control. And we could use this period of time (from point *a* to point *b*) to feed in necessary feedforward control signal.

3. CONTRLLLER DESIGN

Controller design consists of two steps: stabilizing the plant by an inner-loop feedback control Gc and then applying a repetitive learning controller Gf to the closed-loop system to improve the performance through cycle-to-cycle iteration (see

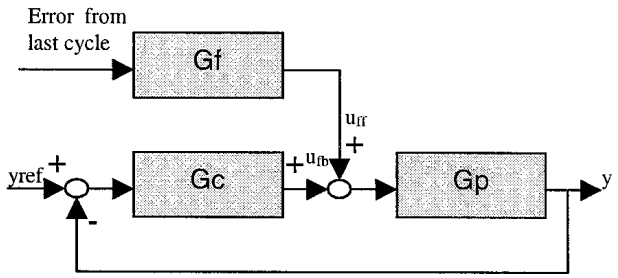

Figure 5. Control Structure

Figure 5).

3.1. Inner-loop Linear Output Feedback Control

A proportional-derivative (PD) controller was used as the inner-loop stabilizing controller. Here we also noticed the second-order mode at 5590 rad/sec. This mode comes from the lash installed between the engine valve and armature. This mode may have significant effect to the system performance as we are pushing the closed-loop crossover-frequency higher to achieve faster response. Therefore a notch filter was cascaded to the PD controller to compress the effect of this mode. It will be demonstrated by experiment in Section 4 that the closed-loop system could go unstable if we take the notch filter out. We end up with a third-order inner-loop controller.

$$Gc = \frac{(Kd \cdot s + Kp)}{(\frac{s}{\omega_4} + 1)} \cdot \frac{(s^2 + 2\xi_2 s + \omega_3)}{(s^2 + 2\xi_3 s + \omega_3)} \qquad \text{(eq. 3-1)}$$

where ω_3 should be a little bit smaller than the plant mode ω_2; ξ_3 could be chosen between 0.7~0.9; and $(s/\omega_4 + 1)$ is a low-pass filter to make the controller causal.

3.2. Cycle-to-Cycle Repetitive Learning Control

We designed our repetitive learning controller by following the synthesis algorithm given by Tsao and Tomizuka. [8] While the algorithm was designed for repetitive control, it could also be applied for the iterative learning control design.

The closed-loop plant the repetitive learning controller "sees" is

$$G_{cp} = \frac{G_p}{1 + G_c G_p} \qquad \text{(eq. 3-2)}$$

The learning control for the (i+1)'th cycle is then given by

$$u_{ff,i+1}(k) = Q \cdot (u_{ff,i}(k) + k_r \cdot M \cdot e_i(k)) \qquad \text{(eq. 3-3)}$$

where $\{e_i(k)\}$ is the error sequence from the i'th cycle; $\{u_{ff,i}(k)\}$ is the feedforward control sequence from the i'th cycle; M is a stable invert of the closed-loop plant G_{cp} with zero phase-error; k_r is a gain to adjust the converging speed; Q is a low-pass filter to maintain the robust stability of the repetitive learner controller.

4. EXPERIMENTAL RESULTS

4.1. Experimental System Setup

Two Pulse Width Modulator (PWM) amplifiers with two DC power supplies drive the two magnet coils of the EMCV. The maximum supply voltage is limited to 42V to simulate the available voltage on a vehicle in the future. A Texas Instrument Digital Signal Processing (DSP) board controls the voltage across each coil in real-time through an I/O board. The sampling frequency was chosen to be 20KHz. The engine valve position is measured by a laser position sensor. The laser sensor outputs a pulse every 0.6328μm. This pulse sequence is then sent back to DSP board through the encoder channel of the I/O board. Current was also monitored although it was not used for control. A personal computer (PC) was used to download program into DSP (see Figure 6).

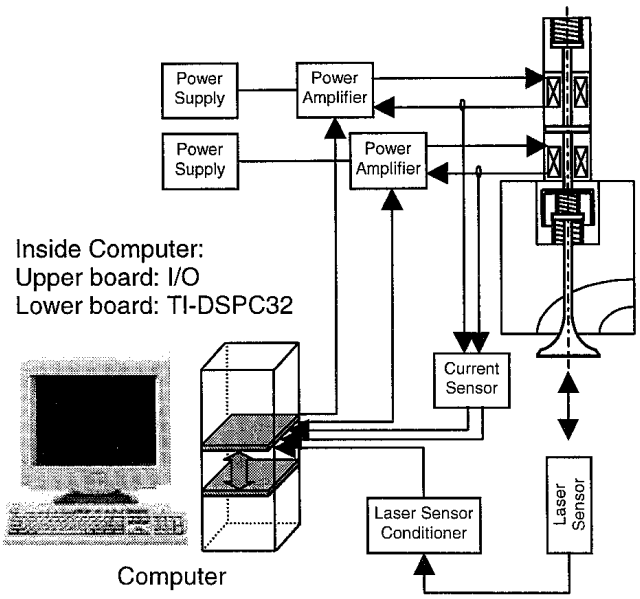

Figure 6. Experimental System Set-up

4.2. Open-loop Repeatability Test

The first stage of this experiment was to excite the system for 50 cycles with pure open-loop pulses and record the seating velocity of each cycle. Different levels of input pulse were tested. It was observed that sometimes the valve closes and sometimes it does not, if the energy put into the system is not high enough. This is because the open-loop system is unstable and therefore is sensitive to perturbations. The repeatability test shows that the lowest seating velocity we may achieve on our experimental system by open-loop control with the valve closed every time is 0.2-0.5 m/s (see Figure 7). [4] This demonstrates that feedback control is necessary to reduce sensitivity and improve repeatability.

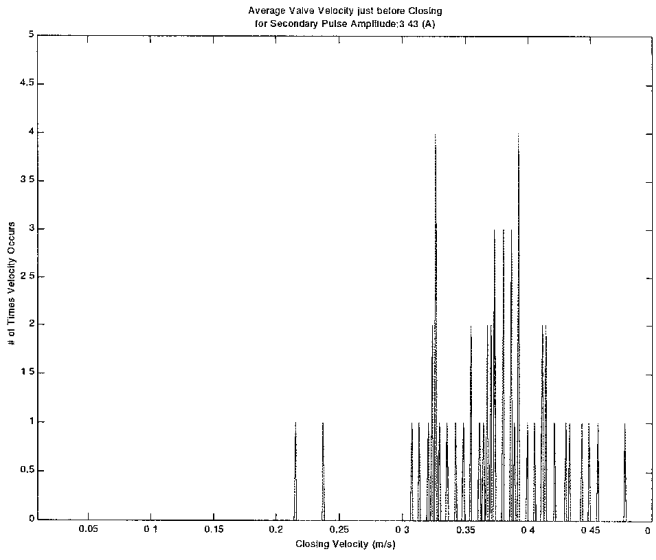

Figure 7. System Repeatibility Test

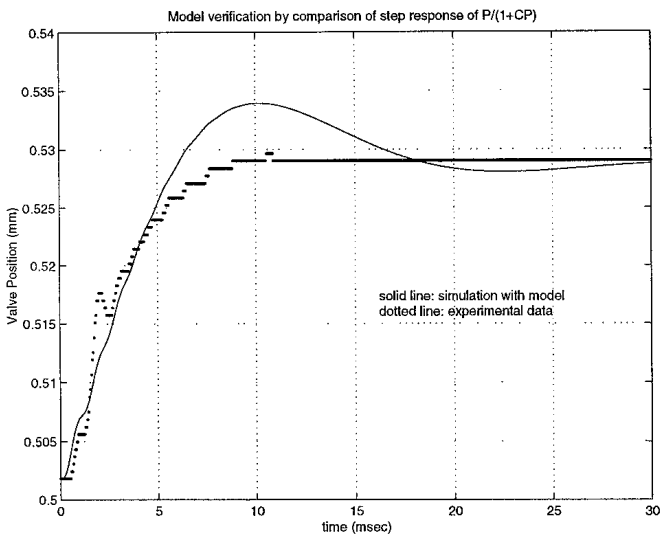

Figure 8. Model Verification

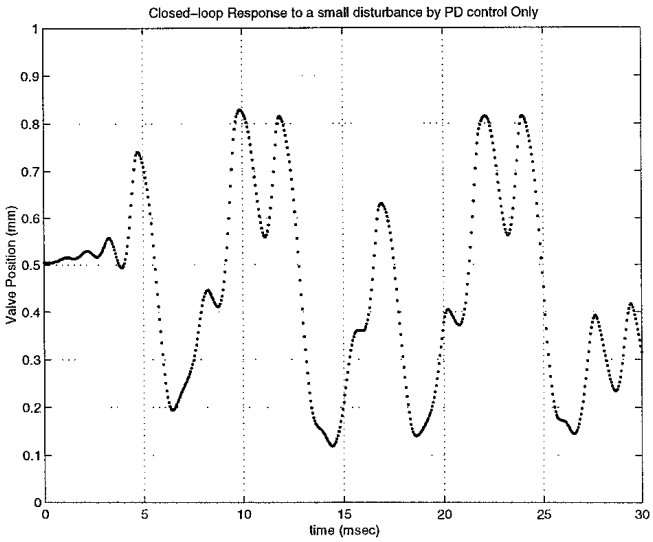

Figure 9. Response after Removing Notching Filter

4.3. Plant Model Verification

We conducted a test to verify our plant model. In this test we first hold the engine valve at some position close to valve seat by using the feedback controller we designed. Then we gave a step-disturbance at the input of the plant. We compared this response to the simulation result using our plant model (see Figure 8). The test result matches simulation result in the sense of the same response-time and steady-state value.

We also demonstrated what could happen if we ignored the dynamic effect of the lash between engine valve and armature. The existence of the high frequency mode around 5600 rad/sec is due to the dynamic effect of lash spring (k_2) and the electromagnet effect (G_1). If we simplify our model by neglecting the dynamic effect of lash, then we will not see this high frequency mode. Based on the simplified model, the PD control we designed before should be able to stabilize the system without the help of notch filter. However, experimental result shows that the high frequency model gradually shows up in the response and eventually drives the closed-loop system unstable. (See Figure 9)

4.4. Control Implementation

At the first step we wanted to see the track performance with feedback control only. Figure 10 shows the test result. As the error starts accumulating, the valve actually "backs off" a little bit before the feedback controller generates enough current to hold it. Then the valve was slowed down and gradually closed. The seating speed is much smaller than 0.05 m/sec. However, it takes about 10 ms for the valve to close tightly. The valve response could not follow the designed trajectory when the valve is getting close to the seat.

During the next stage, we started the iterative learning process to see how much improvement we might get. Figure 11 shows the root mean square of the error summation at each cycle during the iterative learning process. At the beginning of the iterative process, the tracking error gets smaller. However, at some point the error turns bigger. Therefore, we should stop iterative learning process at this point and use the tuned learning control signal as feedforward control.

At the last step we conducted a repeatability test by applying the tuned feedforward control to our feedback system for 50 cycles. Then we plot all the traces together on the same plot to see how repeatable this control system is. This plot is shown in Figure 12. The maximum deviation along these traces is less than 0.1 mm. Therefore we conclude that the response of the closed-loop control system is quite repeatable.

CONCLUSION AND FUTURE WORK

The plant model we obtained is demonstrated valid by experimental verification. The dynamic effect of lash between engine valve and armature is significant and therefore should not be neglected during control design. A linear output feedback controller is able to stabilize the plant around seating position with the limitation of 42V of supply voltage. The seating speed is less than 0.05 m/s for every cycle. However, the output response does not follow the desired trajectory quite well because the feedback controller we designed is kind of conservative due to the existence of the significant nonlinearity in the plant. It helps improving the performance in the sense of following the desired trajectory by adding a repetitive learning feedforward control. However, it still takes about 10 ms for the valve to close tightly, which might not be acceptable on a vehicle engine. In the future work a nonlinear feedback controller may be considered in this situation to improve the control performance and reduce the length of the seating tail.

REFERENCE

[1] Butzmann, S., Melbert, J., and Koch, A., "Sensorless Control of Electromagnetic Actuators for Variable Valve Train," SAE Paper 2000-01-1225

[2] Hoffmann, W., and Stefanopoulou, A., "Valve Position Tracking for Soft Land of Electromechanical Camless Valvetrain," 3rd IFAC Conference Advances in Automotive Control, 2001

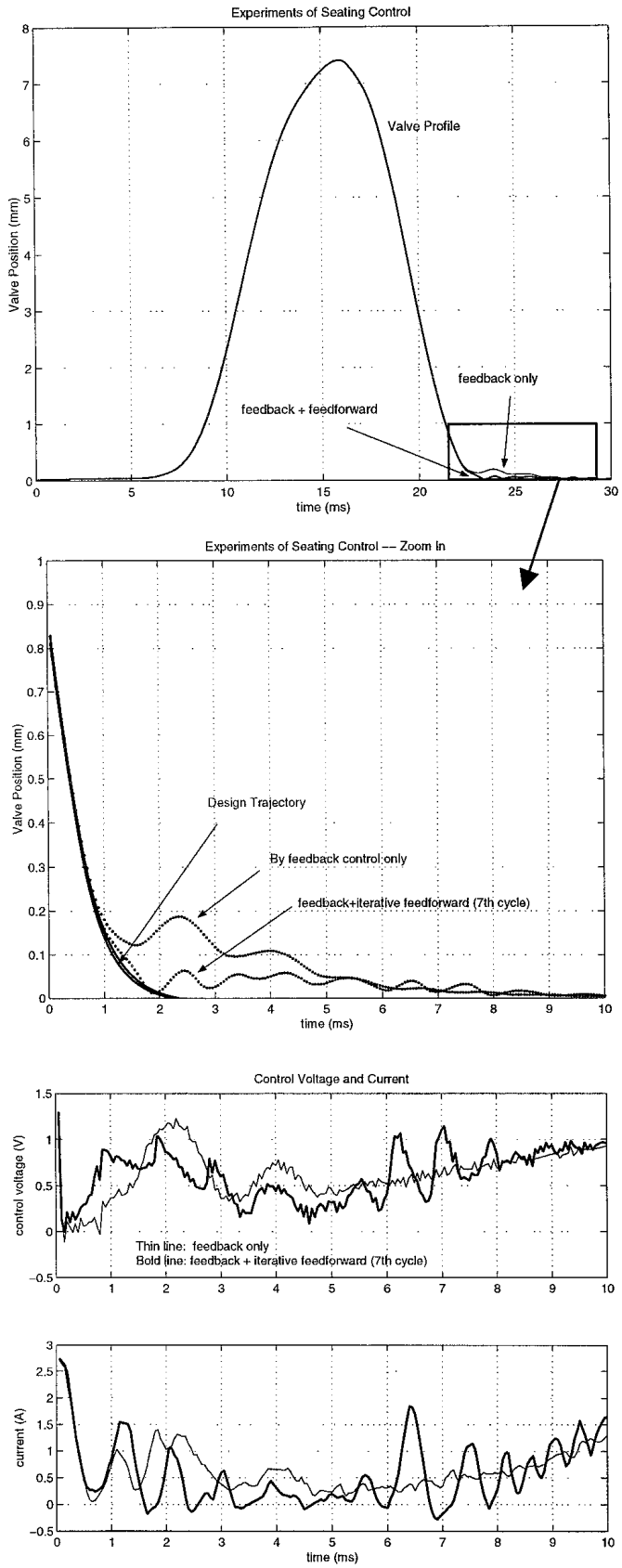

Figure 10. Control Implementation

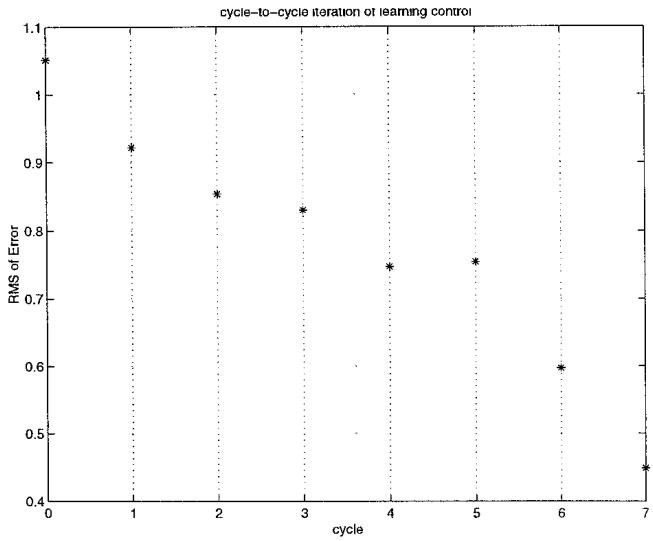

Figure 11. Error Reduction during Learning Control Iteration Process

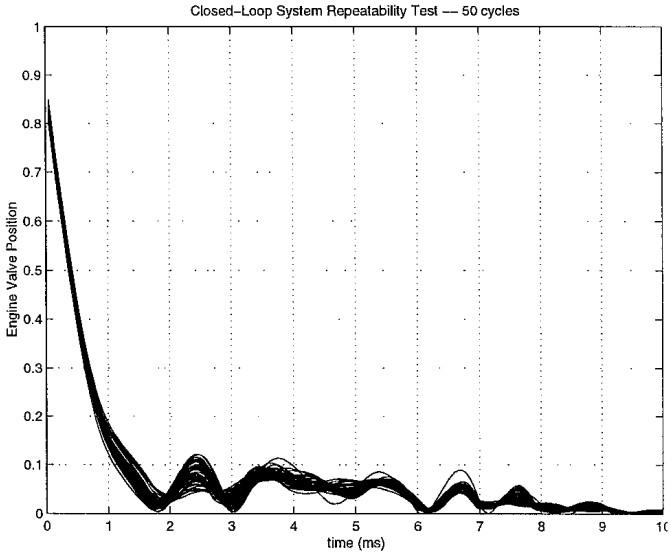

Figure 12. Closed-Loop System Repeatability Test

[3] Schechter, M., and Levin, M., "Camless Engine," SAE Paper 960581, 1996.

[4] Stubbs, A., "Modeling And Controller Design Of An Electromagnetic Engine Valve," MS Thesis, University of Illinois at Urbana-Champaign, 2000

[5] Tai, C., Tsao, T-C., and Levin, M., "Nonlinear Adaptive Feedforward Control of an Electrohydraulic

[6] Camless Valvetrain", American Control Conference, 2000

[7] Tomizuka, M., Tsao, T-C., and Chew, K-K., "Analysis and Synthesis of Discrete-Time Repetitive Controllers," Journal of Dynamic Systems, Measurement, and Control, 1989

[8] Tsao, T-C., and Tomizuka, M., "Robust Adaptive and Repetitive Digital Tracking Control and Application to a Hydraulic Servo for Noncircular Machining," Transactions of ASME, 1994

[9] Wang, Y., Stefanopoulou, A., Haghgooie, M., Kolmanovsky, I., and Hammoud, M. "Modelling of an Electromechanical Valve Actuator for a Camless Engine," 5th International Symposium on Advanced Vehicle Control, Ann Arbor, Michigan USA, 2000